Clays and Clay Minerals, Vol. 46, No. 2, 167–177, 1998.

PEDOGENIC FORMATION OF HIGH-CHARGE BEIDELLITE IN A VERTISOL OF SARDINIA (ITALY)

DOMINIQUE RIGHI[1], FABIO TERRIBILE[2] AND SABINE PETIT[1]

[1] "Hydrogéologie, Argiles, Sols et Altérations", UMR CNRS 6532, Faculté des Sciences, 86022 Poitiers, France
[2] CNR-ISPAIM, PO Box 101, 80040 San Sebastiano al Vesuvio, Napoli, Italy

Abstract—The fine clay (<0.1 μm) fraction of a clayey soil (Vertisol) from Sardinia (Italy) was studied by means of X-ray diffraction (XRD), Fourier transform infrared (FTIR) spectroscopy, cation exchange capacity (CEC) and surface area measurements. Smectites were the dominant clay minerals both in the parent material and the soil horizons. The magnitude and location of the smectites' layer-charges were analyzed using the Hofmann & Klemen effect (suppression of the octahedral charge following lithium-saturation and heating). The amount of montmorillonite layers was evaluated by measuring the reduction of total surface area and CEC after suppression of octahedral charges and subsequent collapse of montmorillonite interlayers. Reduction of total surface area and CEC after fixation of K and irreversible collapse of interlayers were used to quantify high-charge layers before and after the suppression of octahedral charges. This allowed us to evaluate the amount of tetrahedral high-charge layers. The smectites in the parent material were montmorillonitic–beidellitic mixed layers and exhibited a small proportion of high-charge layers; in particular, layers with a high tetrahedral charge were a very minor component. In the upper soil horizons, the amount of montmorillonitic layers decreased whereas the amount of smectite layers with a high tetrahedral charge increased. FTIR spectroscopy indicated more Fe for Al substitution in the smectites of the soil horizons than in the smectites of the parent material. The results suggested that octahedral charged smectite layers (montmorillonitic) were altered, whereas high-charge beidellitic layers were formed in this soil environment characterized by rather high pH (>8.0).

Key Words—Beidellite, High-charge Smectite Layers, Illite–Smectite Mixed Layers, Italy, Smectite, Soil, Vertisol.

INTRODUCTION

It is well established that beidellites are more common in soil environments, whereas montmorillonites are more typical of geologic materials (Wilson 1987). Moreover, high-charge beidellites were reported as the dominant clay mineral in the highly smectitic soils known as Vertisols (Rossignol 1983; Badraoui et al. 1987; Badraoui and Bloom 1990; Bouabid et al. 1996). Soil beidellites are thought to exist as the weathering product of micas and chlorites, because these already have the tetrahedral substitution required for the beidellite structure. The evidence for the formation of smectites from soil solution is difficult to establish. According to Borchardt (1989), beidellites would be crystallized from soil solutions if the pH is less than 6.7, in which case exchangeable Al is present, whereas montmorillonites would be formed in base-saturated soils with low organic matter content and high pH (>6.7), which is the case in Vertisols. However, Kounetsron et al. (1977) showed that beidellite was formed in a Vertisol from the weathering of mica through dissolution and recrystallization processes rather than by simple tranformation of the mica structure.

Righi et al. (1995) described the pedogenic alteration of low- to high-charge beidellites in a Vertisol from South Italy. High-charge beidellites were produced through pedogenic alteration of low-charge smectites in a soil environment characterized by high pH (pH = 8–9) and soil solutions that concentrate with evaporation. Either solid-state reorganization or dissolution-recrystallization were possible mechanisms for producing more Al for Si substitutions in the tetrahedral sheet. The purpose of the present paper was to provide additional results to substantiate the same process in a Vertisol from another location in Italy. The magnitude and distribution of the smectite layer-charge, either in the tetrahedral or in the octahedral sheets, was investigated to address the problem of montmorillonite and beidellite stability in this soil environment. Clay minerals exhibit structural permanent surface charge (related to layer charge) and pH-dependent charge. For 2:1 layer-type clay minerals the structural charge is the greater component of the clay surface charge, which is probably the most important property affecting the chemical and physical behavior of soils and is ultimately related to soil fertility.

SOIL MATERIAL

The selected Vertisol (Typic Pelloxerert, Soil Survey Staff 1994) is located near the village of Suelli (Cagliari) in Sardinia, Italy. The geological substratum in this area is part of a large Miocene formation which consists of marls, arenaceous marls and marl calcarenites. The area covers a large plateau which was extensively eroded. The present landscape consists of few relicts of the plateau and rounded hills, which are

Table 1. Characteristics of the soil horizons clay (<2 μm), $CaCO_3$, OM (organic matter) as percent of 105 °C dried soil.

Soil horizon	Clay	OM	$CaCO_3$	pH (H_2O)	CEC	Ca %CEC	Na %CEC	Mg %CEC	K %CEC
Ap	62.4	2.13	0.1	8.3	33.5	74.9	4.2	17.9	3.0
Bss1	61.0	1.82	0.8	8.1	32.5	71.1	5.8	20.3	2.8
Bss2	61.2	1.26	1.9	8.5	33.6	59.2	7.4	31.5	1.8
Bss/Ck	63.0	0.77	3.8	8.6	28.9	47.4	8.3	42.2	2.1
Ck	48.5	0.33	39.2	8.7	13.1	37.4	9.9	51.1	1.5

CEC: $cmol_c\ kg^{-1}$; Ca, Na, Mg, K: exchangeable cations.

interconnected by means of concave slopes forming large and small basins filled with fine colluvial materials. The study site was selected at the foot of a short concave slope of about 150 m length with a mean slope gradient of about 5%. In this topographic setting, soils were the deepest and exhibited the best vertic characteristics. A short description of the studied soil is given below, and analytical data are presented in Table 1. Munsell colors are for the moist sample.

0–40 cm: Ap, very dark grey (10YR3/1) clay, very friable, fine granular and fine to coarse subangular blocky structure, slight HCl effervescence, regular clear boundary;

40–120 cm: Bssl, black (10YR2/1) clay, firm, strong coarse angular blocky structure with wedge-shaped peds, large peds have slickensides, slight HCl effervescence, smooth gradual boundary;

120–140 cm: Bss2, black (10YR2/1) clay, very firm, very coarse angular blocky structure with wedge-shaped peds, larger peds have distinct slickensides, slight HCl effervescence, undulate clear boundary;

140–175 cm: Bss/Ck, very dark greyish brown (10YR3/2) clay, very firm, very coarse angular blocky and massive structure, few and very large slickensides, strong HCl effervescence, regular gradual boundary;

>175 cm: Ck, olive (5Y4/3) clay, very firm, massive structure, strong HCl effervescence.

Two additional soil horizons (Ap, 0–10 cm and C, >30 cm) were sampled from a shallow eroded soil located at the top of the slope in order to characterize material that could be added to the studied Vertisol through erosion and deposition by colluvial process.

METHODS

The silt and clay fractions were obtained from the soil horizons by sedimentation after destruction of organic matter with dilute H_2O_2 buffered with Na-acetate. Dispersion was done in a NaOH solution at pH 9. No treatment for dissolution of calcium carbonate was used to avoid possible alteration of clay minerals induced by acidification of the medium. The fine clay fraction (<0.1 μm) was obtained from the clay (<2 μm) fraction using a Beckman J2-21 centrifuge equiped with the JCF-Z continuous flow rotor. XRD diagrams were obtained from parallel-oriented specimens using a Philips diffractometer with Fe-filtered Co$K\alpha$ radiation. Pretreatment of the specimens included Ca saturation and solvation with ethylene glycol.

The Hofmann and Klemen effect (1950), which is the suppression of the octahedral charge in dioctahedral smectites after lithium-saturation and heating at 300 °C, was used to distinguish octahedral from tetrahedral charged smectite layers. The conventional treatment was modified by adding a back-saturation step with Ca after the heating sequence. In such conditions smectite layers with a minimum residual tetrahedral charge were expected to re-expand when solvated with ethylene glycol, whereas only smectite layers with no (or very low) tetrahedral charge (ideal montmorillonite) would remain unexpandable by annulation of their octahedral charge. This procedure actually does not distinguish between montmorillonite and beidellite (and nontronite) according to the conventional arbitrary dividing point (50% tetrahedral charge); rather, it distinguishes between ideal montmorillonite (no tetrahedral charge) and other tetrahedrally charged dioctahedral smectites.

High-charge smectite layers were identified on the basis of irreversible collapse of interlayers following fixation of K. Briefly, the fine clay fraction was K-saturated, heated overnight at 110 °C and then back-saturated with Ca, ethylene glycol solvated and submitted to XRD. The loss of expansibility following this treatment was attributed to irreversibly collapsed high-charge layers. The treatment was also applied to lithium-treated fine clay fractions. In such conditions, the loss of expansibility was attributed to high-charge layers with the charge located in the tetrahedral sheet only.

The diffractograms were recorded numerically by a DACO-MP recorder associated with a microcomputer using the Diffrac AT software (SOCABIM). The NEWMOD© program (Reynolds 1985) was used to simulate XRD patterns and to provide a basis for the interpretation of experimental XRD patterns.

CEC was measured with the procedure of Anderson and Sposito (1991), which distinguished between accessible structural permanent charge and variable charge. The procedure was used before and after the fine clay fraction was submitted to the lithium-treatment. The reduction of the CEC after the lithium-treatment was assumed to represent the octahedral charge.

https://doi.org/10.1346/CCMN.1998.0460207 Published online by Cambridge University Press

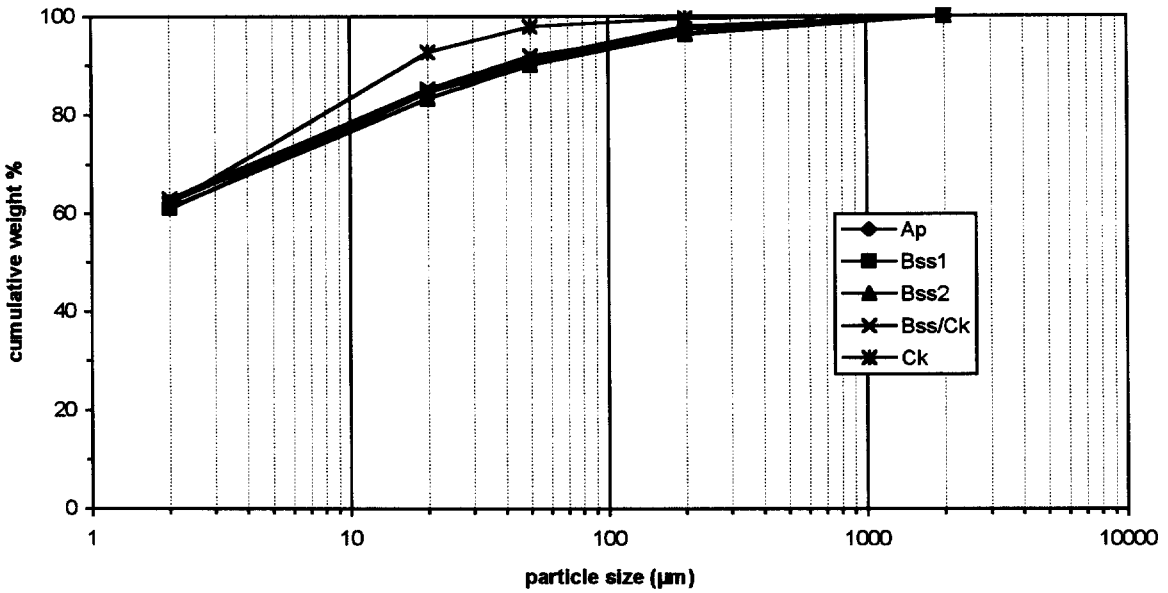

Figure 1. Cumulative grain size distribution curves.

The CEC was also measured after the fine clay fraction was K-saturated and heated at 110 °C. In this case, the CEC was obtained with a conventional exchange method (Righi et al. 1995). The reduction of the CEC after this treatment was assumed to represent the fraction of layer-charge neutralized by irreversibly fixed K. The K-saturation and heat treatment were applied on fine clay fractions previously submitted to the lithium-treatment (suppression of the octahedral charge). Following this procedure, smectite layers with high density of tetrahedral charges (irreversibly collapsed) might be distinguished from smectite layers with low density of tetrahedral charges (re-expanded upon ethylene glycol solvation).

Total chemical analyses were performed on the bulk soil (<2 mm) and fine clay (<0.1 µm) fraction according to the procedure described by Jeanroy (1972). Silicon, Al, Fe, Ti, Mg, Ca, Na and K were analyzed by atomic absorption spectrometry.

Total and external surface areas were measured according to the ethylene glycol monoethyl ether (EGME) (Heilman et al. 1965) and Brunauer–Emmett–Teller (BET) techniques, respectively.

FTIR spectroscopy was performed on KBr disks prepared by mixing 1 mg sample with 300 mg KBr and pressing at 13 kg cm^{-2}. FTIR spectra were recorded using a Nicolet 510 spectrometer.

RESULTS

Soil Analysis

The cumulative grain size distribution curves computed for the 2–2000 µm portion of the 5 horizons were very similar (Figure 1). All the horizons were heavy clays with more than 60% of the particles in the <2 µm fraction (Table 1). The coarse silt and sand fractions were always minor fractions, less than 15% of the whole soil material. Calcium carbonate was present in increasing amounts from the Ap horizon (0.1%) to the Ck horizon (39.2%). The pH in H_2O of soil horizons was about 8.2 in the 2 upper horizons (Ap, Bssl) and higher in the deeper horizons (8.5 to 8.7). The CECs of the soil horizons were between 13.1 and 33.6 $cmol_c\ kg^{-1}$ where exchangeable Mg and Na increased and K and Ca decreased with depth.

Total chemical analysis of the bulk soil material of the various horizons (Table 2) gave similar values throughout the profile, indicating chemically homogeneous materials in the parent material and the soil horizons.

Table 2. Total analyses of the bulk soil samples (<2 mm) as percent of 105 °C dried sample.

Sample	SiO_2	Al_2O_3	Fe_2O_3	MnO	MgO	CaO	Na_2O	K_2O	TiO_2	LOI
Ap	62.51	11.21	4.68	0.11	1.50	1.50	1.12	2.00	0.61	12.96
Bss2	63.12	11.40	4.53	0.10	1.61	1.64	1.11	1.83	0.59	12.08
Bss/Ck	62.75	11.10	4.69	0.11	1.79	1.88	1.04	1.84	0.59	12.40
Ck	63.90	11.48	4.74	0.08	2.50	1.41	1.15	2.01	0.65	10.48

LOI: loss on ignition. (CaO percentages were corrected with reference to calcium carbonate content.)

https://doi.org/10.1346/CCMN.1998.0460207 Published online by Cambridge University Press

Table 3. Total analyses of the fine clay (<0.1 μm) fraction of the studied horizons.

Sample	SiO_2	Al_2O_3	Fe_2O_3	MnO	MgO	CaO	Na_2O	K_2O	TiO_2	LOI
Ap	51.15	18.39	9.80	0.10	2.54	0.33	0.88	2.93	0.47	13.40
Bss2	51.44	17.98	9.56	0.05	2.63	0.38	0.81	2.75	0.58	13.60
Ck	50.89	18.75	8.76	0.02	3.20	0.37	0.74	2.43	0.58	14.30

LOI: loss on ignition as percent of 105 °C dried sample.

Fine Clay Fraction Analyses

Total chemical analysis produced homogeneous results; all the fine clay fractions had a rather constant chemical composition (Table 3). The K_2O contents comprised between 2.43 and 2.93% of the 105 °C dried samples, indicating less than 30% illite or mica layers, as no K-feldspars were present in the samples (Kiely and Jackson 1965). Because no treatment was used to remove iron oxides, Fe_2O_3 contents were assumed to represent silicate iron plus amorphous and/or crystalline forms of iron oxides.

X-ray Diffraction

All the XRD patterns from the fine clay (<0.1 μm) fractions (Figure 2) exhibited the typical diffraction bands of smectitic minerals: intense peak at about 1.52

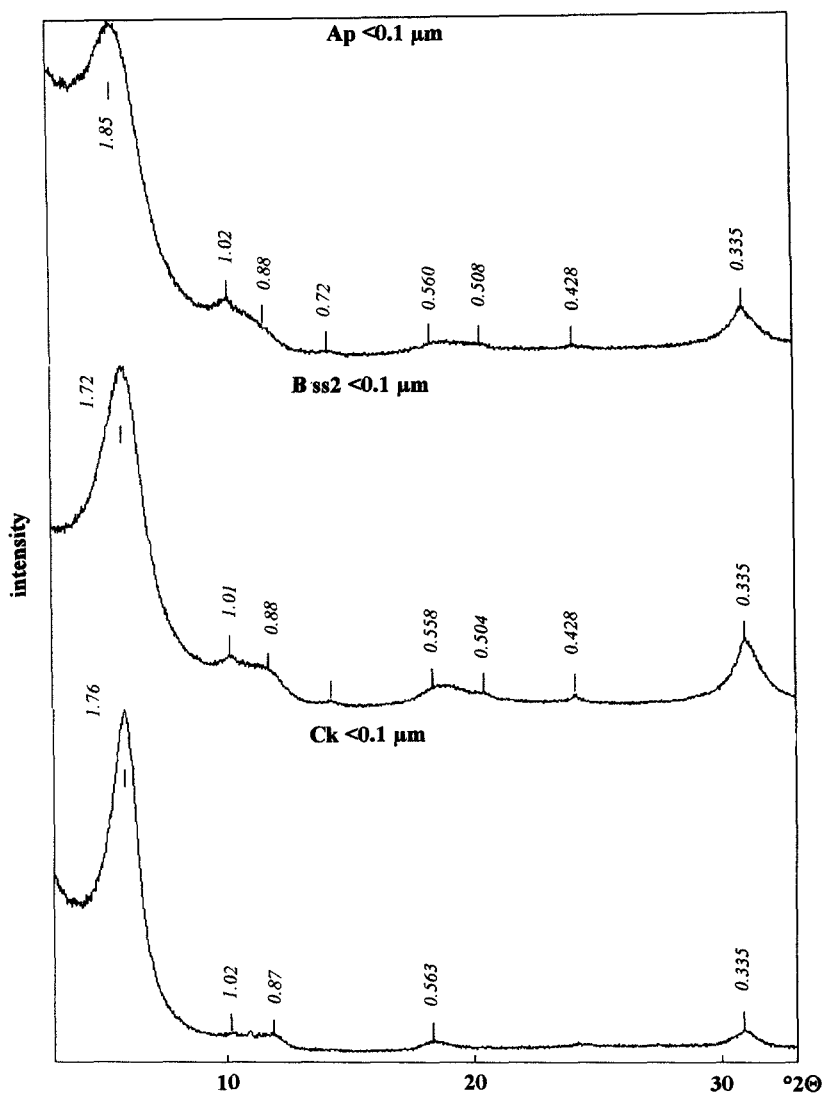

Figure 2. XRD patterns for fine clay (<0.1 μm) fractions. Ca-saturated, ethylene glycol solvated, Co*K*α radiation; *d*(nm).

https://doi.org/10.1346/CCMN.1998.0460207 Published online by Cambridge University Press

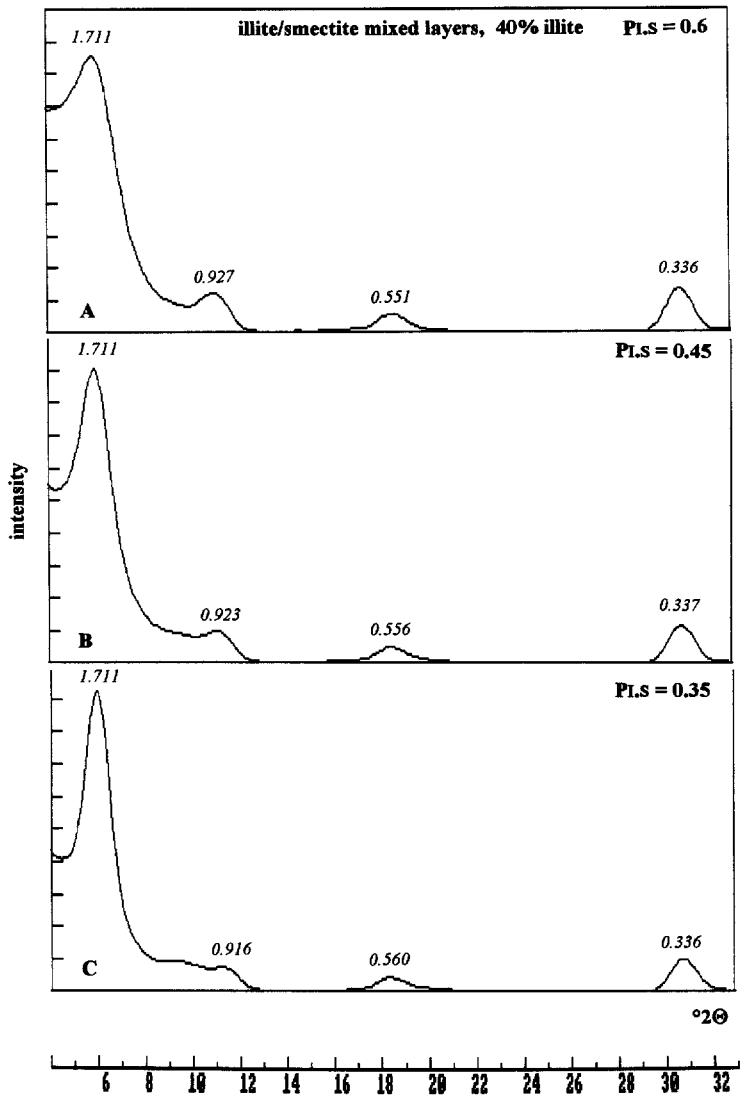

Figure 3. Simulated XRD patterns using NEWMOD© program: A) illite–smectite, random, 40% illite; B) illite–smectite, effect of segregation of illite (I) and smectite (S) layers shown by P1.S = 0.45 (P1.S: probability of having a smectite layer following an illite layer. P1.S = 0.6 represents random condition, smaller P1.S represents increasing segregation); C) illite–smectite, effect of segregation shown by P1.S = 0.35. Coherent scattering domain size: 4–6 layers; *d*(nm).

nm (air-dry, not shown) or 1.72–1.85 nm (ethylene glycol) with higher order at 0.87–0.88, 0.558–0.563 and 0.335 nm. In addition small peaks at 1.01–1.02 nm and 0.504–0.508 nm, attributed to illitic material, are shown on the diagrams from the Bss2 and Ap horizon samples. All the fine clay phyllosilicates were dioctahedral minerals, as indicated by a 060 band at 0.150 nm (not shown). The increase of the intensity ratio of the 001 peak at about 1.70–1.80 nm to the background, downangle from the 001 peak, indicated illite–smectite mixed layers (I–S) with increasing proportion of illitic layers from the Ck to the Ap horizon. Actually, this ratio has been used as a routine determination (known as the "saddle/001" method) of percentage of smectite layers in I–S mixed layers (Inoue et al. 1989). However, the total surface areas and CEC values (see below) were consistent and suggested the same proportion of collapsed and expanded components in the mixed layers from the upper soil horizons and the parent material. Therefore, for the interpretation of XRD patterns, a simulation of the XRD diagrams was made using the NEWMOD© program which, among other facilities, allowed us to simulate the effect of the segregation of illite and smectite layers in an I–S mixed layer. It was possible to simulate the experimental patterns for I–S mixed layers with 60% smectite (Figure 3). The simulation of the XRD diagram from the Ck horizon required introduction of

https://doi.org/10.1346/CCMN.1998.0460207 Published online by Cambridge University Press

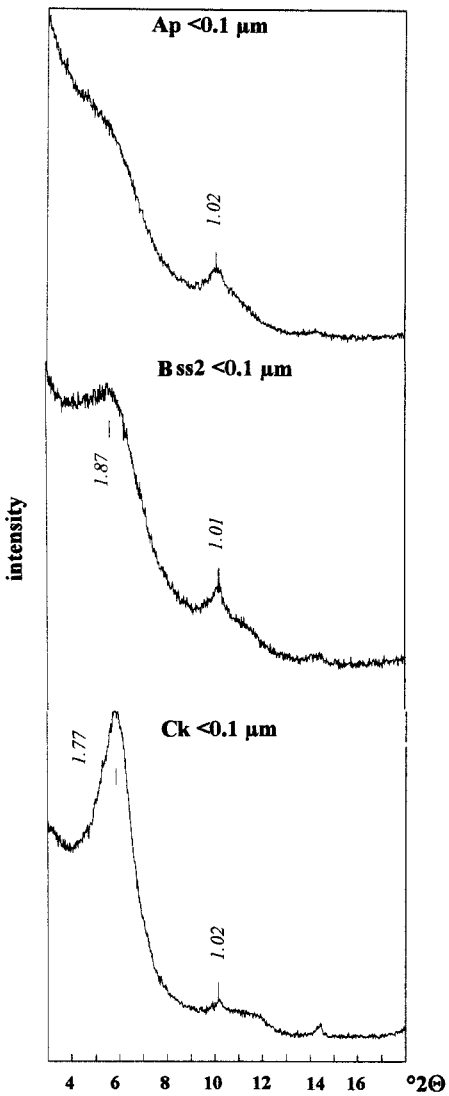

Figure 4. XRD patterns for the fine clay (<0.1 µm) fractions after K-saturation, heating and back-saturation with Ca. Ethylene glycol solvated, Co*K*α radiation; *d*(nm).

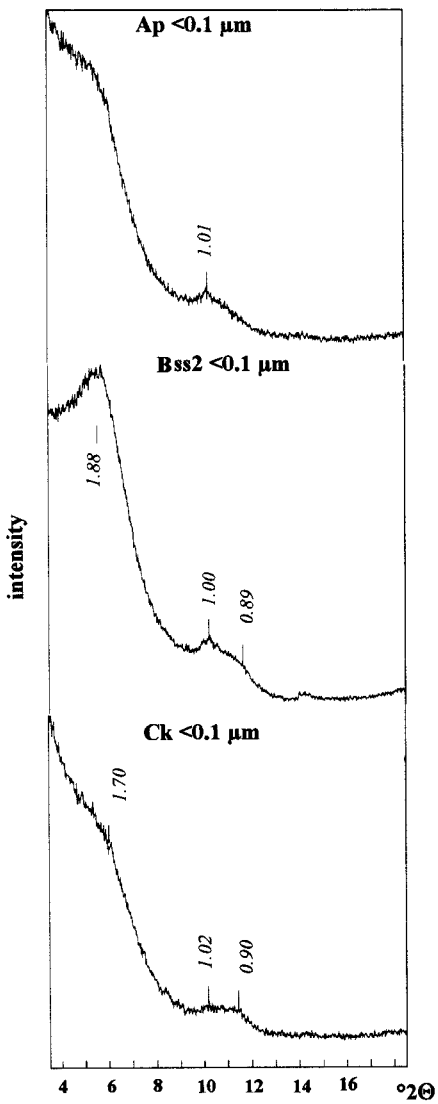

Figure 5. XRD patterns for the fine clay (<0.1 µm) fractions after lithium-saturation, heating at 300 °C and back-saturation with Ca. Ethylene glycol solvated, Co*K*α radiation; *d*(nm).

a rather strong segregation effect (as shown by the probability Pi.s, of having a smectite layer following an illite layer equal to 0.35) not needed for the simulation of the Ap horizon diagram. Thus, in agreement with CEC values and total surface areas, all the soil horizons would contain I–S mixed layers with identical proportion of smectite layers; only the distribution of smectite and illite layers in the stacking sequence would change from one horizon to another. More segregation of the collapsed and expandable layers would be present in the clay crystals of the parent material than in those of the upper soil horizons.

A decrease in the proportion of expandable layers of the fine clay fractions was obtained by the K-saturation and heat treatment (Figure 4), as shown by the increase of the saddle/001 peak ratio.

Following the lithium-treatment, all the fine clay fractions exhibited a partial re-expansion upon ethylene glycol solvation (Figure 5). In response to that treatment, a physical mixture of beidellite and montmorillonite would produce 2 XRD peaks, one near 1.70 nm for expanded beidellite and a second one near 0.97 nm for collapsed montmorillonite. Compared to the untreated fine clay fractions (see Figure 2), no increase of the diffracted intensity at about 0.97 nm that would indicate discrete particles of octahedral charged smectite layers was observed for the studied samples. Moreover, the XRD patterns were those of collapsed

https://doi.org/10.1346/CCMN.1998.0460207 Published online by Cambridge University Press

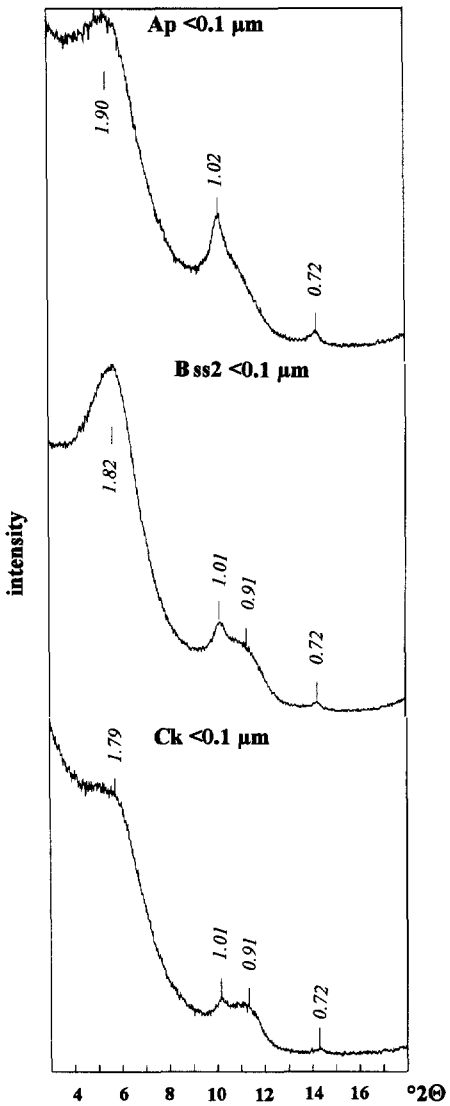

Figure 6. XRD patterns for the lithium-treated fine clay (<0.1 μm) fractions after K-saturation, heating and back-saturation with Ca. Ethylene glycol solvated, Co$K\alpha$ radiation; d(nm).

(montmorillonitic) and expanded (beidellitic) mixed layers, as shown by the high saddle/001 peak ratio. Thus, the smectite component in the parent material and the soil horizons exhibited heterogeneous charge distribution and could be seen as a random interstratification of beidellitic and montmorillonitic layers.

Following the K-saturation and heat treatment applied to the lithium-treated samples, the XRD pattern of the fine clay fraction from the parent material was only slightly affected. Only a small increase of the relative intensity of the peak at 1.01 nm was observed (Figure 6). The relative intensity of the peak at 1.02 nm was increased and a more pronounced change was observed for the XRD patterns of the fine clay fractions from the upper soil horizons compared with the original lithium-treated sample (see Figure 5).

Surface Area Measurements

The external surface areas (ES) of the fine clay fraction in the soil horizons decreased from 159 (Ap horizon) to 141 (Bss2 horizon) and 102 $m^2\ g^{-1}$ (Ck horizon) (Table 4). The total surface areas (TS) were relatively similar and comprised between 536 (Ap horizon) and 565 (Ck horizon) $m^2\ g^{-1}$. By subtraction of the external from the total surface area (TS − ES), internal surface areas (IS) were estimated to be 377 (Ap horizon), 420 (Bss2) and 465 $m^2\ g^{-1}$ (Ck).

Following the K-saturation treatment, the total surface area was reduced to 377, 373 and 449 $m^2\ g^{-1}$ for the Ap, Bss2 and Ck horizon samples, respectively (KTS, Table 4). The reduction was attributed to the collapse of high-charge smectite interlayers. Thus, the difference TS − KTS gives the internal surface area of high-charge smectite layers (hc layers, Table 4). It was 159 (Ap horizon) and 188 $m^2\ g^{-1}$ (Bss2 horizon) and 116 $m^2\ g^{-1}$ (Ck horizon), indicating more collapsed high-charge layers in the upper soil horizons.

Following the lithium-treatment, the total surface area was reduced to 431, 466 and 344 $m^2\ g^{-1}$ for the Ap, Bss2 and Ck horizon samples, respectively (LiTS, Table 4). The reduction was attributed to the collapse of the montmorillonitic smectite layers and the difference TS − LiTS was assumed to represent the internal surface of these layers (Mt layers, Table 4) which was 221 $m^2\ g^{-1}$ for the Ck, 95 $m^2\ g^{-1}$ for the Bss2 and 105

Table 4. Surface areas ($m^2\ g^{-1}$) for the fine clay fraction of the studied horizons.

Horizon	TS (egme)	ES (BET)	LiTS	KTS	K/LiTS	IS (TS − ES)	Mt layers	hc layers	hc Bd layers
Ap	536	159	431	377	374	377	105	159	57
Bss2	561	141	466	373	401	420	95	188	65
Ck	565	102	344	449	328	463	221	116	16

TS: total surface area; ES: external surface area; LiTS: total surface area of Li-treated samples; KTS: total surface area of K-saturated and heated samples; K/LiTS: total surface area of K-saturated and heated Li-treated samples; IS: internal surface area; Mt layers = (TS − LiTS): internal surface area of collapsed layers after Li-treatment (montmorillonitic); hc layers = (TS − KTS): internal surface area of high charge layers; hc Bd layers = (LiTS − K/LiTS): internal surface area of layers with high tetrahedral charge (beidellitic).

https://doi.org/10.1346/CCMN.1998.0460207 Published online by Cambridge University Press

Table 5. Cation exchange capacities ($cmol_c\ kg^{-1}$) of the fine clay fraction of studied horizons.

Horizon	apc	vc	CEC	Li-apc	Li-vc	Li-CEC	oct-apc	K-CEC	Δ CEC
Vertisol									
Ap	53.1	18.2	71.3	32.8	19.8	52.6	20.3	51.0	20.3
Bss2	51.5	18.3	69.8	33.7	20.2	53.9	17.8	49.1	20.7
Ck	52.3	16.1	68.4	23.5	16.9	40.4	28.8	55.5	12.9
Eroded soil									
Ap	—	—	71.8	—	—	37.0	34.8	—	—
C	—	—	67.3	—	—	28.0	39.3	—	—

apc: accessible permanent charge; vc: variable charge; CEC = (apc + vc); Li-apc: accessible permanent charge of the Li-treated samples = accessible tetrahedral charge; Li-vc: variable charge of Li-treated samples; Li-CEC: CEC of Li-treated samples; oct-apc: octahedral accessible permanent charge = (apc − Li-apc); K-CEC: CEC of K-saturated and heated samples; Δ CEC = (CEC − K-CEC). —: not measured.

$m^2\ g^{-1}$ for the Ap horizon. Thus, the proportion of smectite layers collapsed by the lithium treatment (montmorillonitic layers with no or very low tetrahedral charge) in the parent material was about twice the value of the upper soil horizons.

Following K-saturation and heat treatment applied on lithium-treated samples, the total surface area was reduced to 374, 401 and 328 $m^2\ g^{-1}$ for the Ap, Bss2 and Ck horizon samples, respectively (K/LiTS, Table 4). The difference LiTS − K/LiTS was assumed to measure the internal surface area of high-charge smectite layers with the layer charge located in the tetrahedral sheet only (hc Bd layers, Table 4). This area increased from 16 $m^2\ g^{-1}$ for the Ck horizon to 65 $m^2\ g^{-1}$ for the Bss2 horizon and 57 $m^2\ g^{-1}$ for the Ap horizon, indicating more irreversibly collapsed layers (layers with high tetrahedral charge) in the upper soil horizons than in the parent material.

Cation Exchange Capacity

CEC values obtained from the fine clay fractions are given in Table 5. The CEC value was very similar for all the fine clay fractions (68.4 $cmol_c\ kg^{-1}$, Ck horizon, to 71.3 $cmol_c\ kg^{-1}$, Ap horizon). The portion of the CEC attributed to variable charge (vc) was 18.2 $cmol_c\ kg^{-1}$ in the Ap and 16.0 $cmol_c\ kg^{-1}$ in the Ck horizon, whereas an accessible structural permanent charge (apc) of about 52 $cmol_c\ kg^{-1}$ was found for the fine clay fractions from the 3 soil horizons investigated.

The accessible permanent charge located in the tetrahedral sheet was obtained from the fine clay fractions subjected to the lithium-treatment (Table 5). The accessible tetrahedral charge (Li-apc) was smaller for the parent material (23.5 $cmol_c\ kg^{-1}$) than for the upper soil horizons (33.7 $cmol_c\ kg^{-1}$ Bss2 horizon, 32.8 $cmol_c\ kg^{-1}$ Ap horizon), while the reverse was true for the accessible octahedral charge (oct-apc). Only a small increase of the fraction of the CEC attributed to variable charges (Table 5) was observed after the lithium-test, indicating that edges of clay particles were not dramatically altered.

The CEC values of the fine clay fractions were reduced after the K-saturation treatment (Table 5). The reduction of CEC was about 20 $cmol_c\ kg^{-1}$ (30% of the original CEC) for the Ap and Bss2 horizon fine clay fractions and about 13 $cmol_c\ kg^{-1}$ (20% of the original CEC) for the Ck horizon fine clay fraction. More K was fixed in the upper soil horizons than in the parent material.

FTIR Spectroscopy

The FTIR spectra (Figure 7) from all the fine clay fractions established the aluminous character of the smectites (AlOHAl band at 912 cm^{-1}). Substitution of Mg for Al and thus occurrence of charge in the octahedral sheet was shown by the AlOHMg band near 840 cm^{-1}. This band was more intense for the fine clay fraction from the parent material of the Vertisol and the horizons of the shallow eroded upslope soil. In addition, substitution of Fe(III) for Al in the fine clay fraction from the 2 upper soil horizons was demonstrated by the AlOHFe(III) band at 880 cm^{-1}. This band was nearly absent in the spectra from the fine clay fraction of the parent material of the Vertisol and the shallow eroded soil. It was present but very weak for the sample from the Ap horizon of the shallow eroded soil.

DISCUSSION

Particle size distribution and total chemical analysis of the bulk soil gave similar results for each of the soil horizons. The fine silt (2–5 μm) fractions (not shown) from the parent material and the upper soil horizons contained the same mineral suite characterized by mica (peaks at 1.010 and 0.501 nm), quartz (0.427 and 0.335 nm), feldspars (0.380 and 0.320 nm) and kaolinite (0.715 and 0.355 nm). This supports the assumption that before pedogenic alteration took place, the soil parent material was homogeneous, without any lithologic discontinuity. Only calcium carbonate content increased with depth, and may be attributed to pedogenic redistribution. According to topography,

https://doi.org/10.1346/CCMN.1998.0460207 Published online by Cambridge University Press

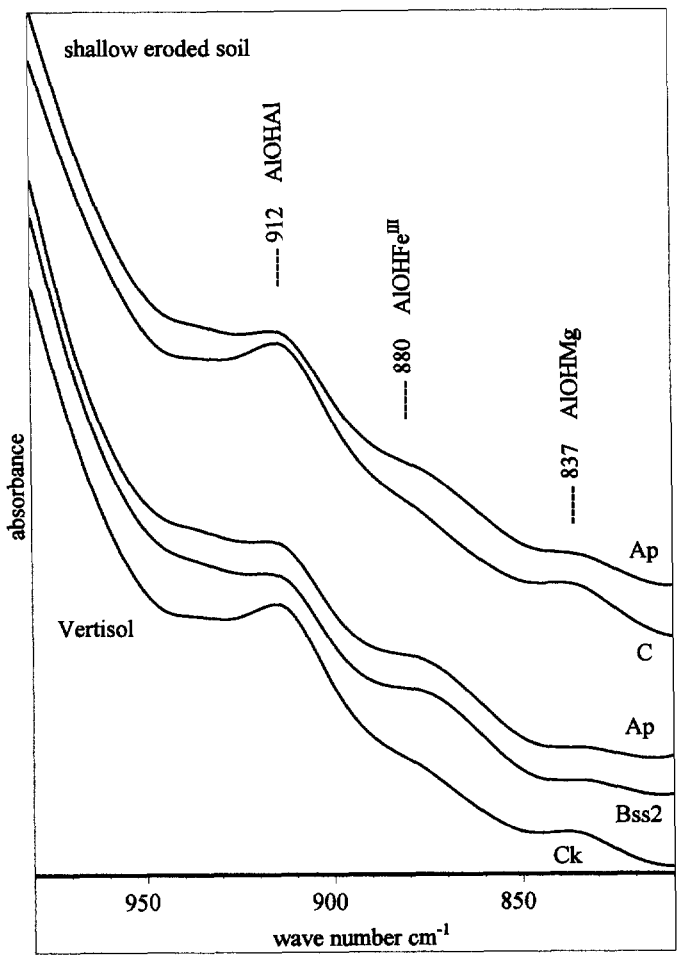

Figure 7. FTIR spectra for the Vertisol and shallow eroded soil fine clay (<0.1 μm) fractions.

the additions of material to the Vertisol from erosion of the upper area of the hills should not be excluded. The fine clay fractions from a shallow eroded upslope soil exhibited similar characteristics to that of the parent material of the Vertisol; the layer charge was dominantly octahedral and the FTIR spectra did not show the AlOHFe(III) band at 880 cm^{-1} which was present in the fine clay fractions from the upper soil horizons of the Vertisol. Consequently, the mineralogical changes observed from the parent material to the upper soil horizons could not be attributed to contamination by colluvial material.

The XRD patterns from the fine clay fractions were characterized by the increase of the saddle/001 peak intensity ratio from the Ck to the Ap horizon. Based on XRD simulated diagrams (Reynolds 1980; Inoue et al. 1989), the increase of this ratio suggested I–S mixed layers with decreasing proportion of smectite layers. However, the total surface area (lower than that attributed to pure smectite, 810 $m^2\ g^{-1}$, (Carter et al. 1965) and CEC values were consistent and suggested the same proportion of collapsed and expandable components in the mixed layers from the upper soil horizons and the parent material. Moreover, the total surface area and CEC values were in good agreement with the results of Środoń et al. (1992) who found that an I–S mixed layer with 60% smectite, as evaluated from XRD, would have a total surface area of 550 $m^2\ g^{-1}$ and a CEC of 70 $cmol_c\ kg^{-1}$. Using computed XRD diagrams, it was possible to simulate the experimental patterns of the 3 samples with I–S mixed layers having the same proportion of smectite layers (60%). Only more segregation of the collapsed and expandable layers would be present in the clay crystals of the parent material than in those of the upper soil horizons. This suggested that the clay minerals in the upper soil horizons did not derive simply by inheritance from the parent material, but rather, new clay crystals with a different distribution of layers in the stacking sequence were formed by pedogenesis.

The fine clay fractions exhibited XRD patterns typical of I–S mixed layers; however, the K_2O contents

https://doi.org/10.1346/CCMN.1998.0460207 Published online by Cambridge University Press

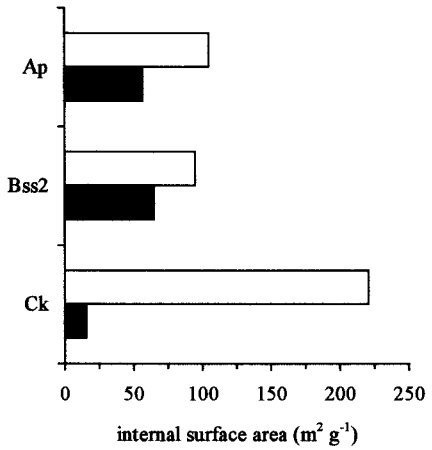

Figure 8. Histograms of internal surface areas for layers with (white bar) a tetrahedral charge <0.24 $mol_c/O_{10}(OH)_2$ (montmorillonitic layers) and layers with (black bar) a tetrahedral charge >0.77 $mol_c/O_{10}(OH)_2$ (high-charge beidellitic layers).

were not high enough to account for the I–S mixed layers with 40% illite identified from the XRD patterns. Therefore, it is likely that a part of these mixed layers were interstratifications of irreversibly collapsed and expandable smectite layers rather than true I–S mixed layers.

The XRD patterns, the reduction of the CEC and the total surface area after K-saturation and heating gave consistent results, suggesting more high-charge smectite layers in the upper soil horizons than in the parent material, as it was previously observed in another Vertisol (Righi et al. 1995). According to Eberl (1980), irreversible K-fixation requires a layer charge of 0.77 $mol_c/O_{10}(OH)_2$, but K could be fixed at lower layer charge if the clay is oven-dry.

The lithium-treatment was used to distinguish smectite layers exhibiting a tetrahedral charge. It was postulated that back-saturation with Ca of the lithium-saturated and heated fine clay fraction would allow any smectite layers with a remaining tetrahedral charge to re-expand upon ethylene glycol solvation, as demonstrated by Jaynes and Bigham (1987). Malla and Douglas (1987) stated that, after lithium-treatment, only smectite layers with a remaining tetrahedral charge higher than 0.24 $mol_c/O_{10}(OH)_2$ could re-expand. Therefore, irreversibly collapsed layers, as measured by the reduction of total surface area, were assumed to be smectite layers with charges located almost exclusively in the octahedral sheet, whereas the smectite layers which re-expanded following the lithium-treatment were assumed to have a tetrahedral charge higher than 0.24 $mol_c/O_{10}(OH)_2$. The reduction of the total surface area was consistent with the reduction of the CEC, both indicating more octahedral-charged smectite layers in the parent material than in the upper soil horizons. Moreover, XRD patterns have shown that tetrahedral-charged layers were interstratified with the octahedral-charged smectite layers and did not exist as separate crystals as it should be expected if the beidellitic smectite layers were formed by weathering of a mica phase.

Compared to the untreated fine clay fraction, far less high-charge smectite layers were found after the lithium-treatment, indicating that a large portion of the tetrahedral-charged layers also had an octahedral charge that contributed to the high-charge behavior and was suppressed by the lithium-treatment. The smectite layers with a high-charge behavior that could be attributed to the tetrahedral charge alone were found essentially in the upper soil horizons, suggesting that the overall increase of the layer charge was located in the tetrahedral sheet. Figure 8 shows the distribution in the different soil horizons of the smectite layers with either a dominant octahedral or a high tetrahedral charge. This shows the mineralogical changes in the studied soil: a decrease of the relative proportion of octahedral-charged smectite layers and an increasing amount of layers with high density of tetrahedral charges. Montmorillonitic smectites would be more affected by weathering than beidellitic smectites that would be more stable in this soil environment.

In soils, high-charge beidellites were often described as the weathering product of micas (Borchardt 1989; Bouabid et al. 1996). In the studied soil, the silt and clay fractions of the parent material and the upper soil horizons contained micas; therefore, their contribution to the formation of smectite layers with high tetrahedral charge should not be excluded. The total chemical analyses of the bulk soil indicated that the soil parent material contained very small amounts of mica, and it is unlikely that the whole mass of tetrahedral charged smectites found in the soil horizons was derived from mica.

The increase of the proportion of smectites with tetrahedral charges in the upper soil horizons was associated with a change of the octahedral composition, as shown by FTIR spectroscopy. The upper soil horizons contained more smectite layers with Fe(III) for Al substitution than the parent material. This strongly suggested that the mineralogical change proceeds through dissolution–recrystallization processes rather than solid-state reorganization.

CONCLUSION

Righi et al. (1995) proposed the hypothesis of formation of high-charge beidellites in Vertisols by increase of tetrahedral substitution as a pedogenic process. The theory was supported by the experimental work of Eberl et al. (1993) that showed the formation of high-charge smectite layers at low temperature and alkaline environment. The present study confirmed the phenomenon: smectites in the upper soil horizons had

more tetrahedral substitutions than the smectites in the parent material. This suggested the pedogenic formation of beidellites in this soil environment.

ACKNOWLEDGMENTS

This study was part of a cooperative program supported by CNR (Italy) and CNRS (France). Programme de Recherche en Coopération sur Conventions Internationales du CNRS, Projet #3187/1997. The authors would like to thank A. Aru, P. Baldaccini and their collaborators for their essential support in choosing and sampling the study site.

REFERENCES

Anderson SJ, Sposito G. 1991. Cesium-adsorption method for measuring accessible structural surface charge. Soil Sci Soc Am J 55:1569–1576.

Borchardt G. 1989. Smectites. In: Dixon JB, Weed SB, editors. Minerals in soil environments, 2nd ed. Madison, WI: Soil Sci Soc Am. p 675–727.

Bouabid R, Bradaoui M, Bloom PR, Daniane M. 1996. The nature of smectites and associated interstratified minerals in soils of the Gharb plain of Morocco. Eur J Soil Sci 47: 165–174.

Bardaoui M, Bloom PR. 1990. Iron-rich high-charge beidellite in Vertisols and Mollisols of the High Chaouia region of Morocco. Soil Sci Soc Am J 54:267–274.

Bardaoui M, Bloom PR, Rust RH. 1987. Occurrence of high-charge beidellite in a Vertic Haplaquoll of northwestern Minnesota. Soil Sci Soc Am J 51:813–818.

Carter DL, Heilman MD, Gonzalez CL. 1965. Ethylene glycol monoethyl ether for determining the surface area of silicate minerals. Soil Sci 100:356–360.

Eberl DD. 1980. Alkali cation selectivity and fixation by clay minerals. Clays Clay Miner 28:161–172.

Eberl DD, Velde B, McCormick T. 1993. Synthesis of illite-smectite from smectite at Earth surface temperatures and high pH. Clay Miner 28:49–60.

Heilman MD, Carter DL, Gonzalez CL. 1965. The ethylene glycol monoethyl ether (EGME) technique for determining soil-surface area. Soil Sci 100:409–413.

Hofmann VU, Klemen R. 1950. Verlust der austauschfähigkeit von lithium-ionen an bentonit durch erhitzung. Zeitung für Anorganische Chemie 262:95–99.

Inoue A, Bouchet A, Velde B, Meunier A. 1989. Convenient technique for estimating smectite layer percentage in randomly interstratified illite/smectite minerals. Clays Clay Miner 37:227–234.

Jaynes WF, Bigham JM. 1987. Charge reduction, octahedral charge, and lithium retention in heated, Li-saturated smectites. Clays Clay Miner 35:440–448.

Jeanroy E. 1972. Analyse totale des silicates naturels par spectrométrie d'absorption atomique. Application au sol et à ses constituants. Chim Anal 54:159–166.

Kiely PV, Jackson ML. 1965. Quartz, Feldspar and Mica determination for soils by sodium pyrosulfate fusion. Soil Sci Soc Am Proc 29:159–163.

Kounetsron O, Robert M, Berrier J. 1977. Nouvel aspect de la formation des smectites dans les vertisols. C R Acad Sci Paris 284:733–736.

Malla PB, Douglas LA. 1987. Problems in identification of montmorillonite and beidellite. Clays Clay Miner 35:232–236.

Reynolds RC Jr. 1980. Interstratified clay minerals. In: Brindley GW, Brown G, editors. Crystal structures of clay minerals and their X-ray identification. London: Miner Soc. p 249–359.

Reynolds RC Jr. 1985. NEWMOD: A computer program for the calculation of one-dimensional diffraction powders of mixed-layer clays. 8 Brook Rd., Hanover, NH 03755: RC Reynolds, Jr.

Righi D, Terribile F, Petit S. 1995. Low-charge to high-charge beidellite conversion in a Vertisol from South Italy. Clays Clay Miner 43:495–502.

Rossignol JP. 1983. Les Vertisols du nord de l'Uruguay. Cah ORSTOM sér Pédol 20:271–291.

Soil Survey Staff. 1994. Keys to soil taxonomy, 5th ed. Blacksburg, VA: Pocahontas Pr.

Środoń J, Elsass F, McHardy WJ, Morgan DJ. 1992. Chemistry of illite/smectite inferred from TEM measurements of fundamental particles. Clay Miner 27:137–158.

Wilson MJ. 1987. Soil smectites and related interstratified minerals: Recent developments. In: Schultz LG, van Olphen H, Mumpton FA, editors. Proc Int Clay Conf; 1985; Denver, CO. Bloomington, IN: Clay Miner Soc. p 167–173.

(Received 4 November 1996; accepted 9 August 1997; Ms. 2827)